

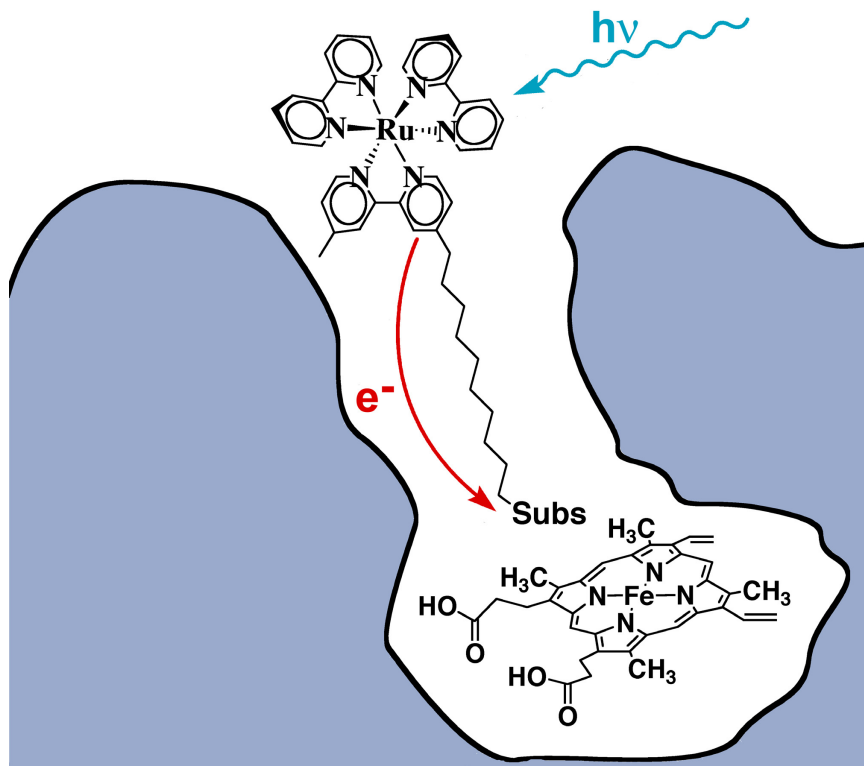
Chapter 1

Introduction

This thesis describes the use of photoactive molecules to study heme enzyme reaction mechanisms and structural dynamics. Our approach has been to attach a photosensitizer to an enzyme substrate by a covalent tether (Figure 1.1). The substrate provides the binding energy and specificity to bring the sensitizer to the target enzyme. Once the sensitizer is bound, a variety of photophysical and photochemical processes may be used to detect the presence of the enzyme, characterize its structure and dynamics, or trigger reactions within it.

Sensitizer-linked substrates (SLS) help to span the orders of magnitude between our sensory experience and chemically relevant lengths (cm vs. nm), times (s vs. ps), and numbers (moles vs. molecules). Förster energy transfer (FET) and photo-triggered electron transfer (ET) occur over nanometer distances, luminescence decay occurs on the pico- to microsecond timescales, and the detection of single fluorescent molecules is now a well-established technique.¹ In addition, the association of the sensitizer with the target enzyme through a substrate or inhibitor has several useful aspects. The sensitizer can act as a spectroscopic probe to characterize the interactions of the target enzyme with small molecules. In addition, the specificity of the enzyme:SLS interaction can potentially provide binding selectivity in chemically complex environments. Because preassociation of the enzyme and sensitizer circumvents the time restraints inherent to bimolecular diffusive reactions, SLS probes can be used to photochemically trigger reactions on the

Figure 1.1. A schematic representation of an SLS:enzyme conjugate. In this example, a ruthenium *tris*-bipyridyl photosensitizer reduces the heme upon excitation with 470 nm light. The substrate moiety (subs) mediates the binding of the SLS to the target enzyme. The linker serves both to connect the sensitizer to the substrate and to mediate electron tunneling from the Ru-diimine to the heme.



submicrosecond timescale. Unlike covalently labeled proteins, the SLS:enzyme conjugate can be formed immediately prior to the experiment, thus circumventing potential complications due to degradation of the enzyme:photosensitizer conjugate.

The remainder of the Introduction serves two purposes. The Background section contains information taken for granted in the remainder of the thesis. The topics covered are: Förster energy transfer, electron transfer theory, ruthenium *tris*-bipyridine photochemistry, enzyme-small molecule interactions, cytochrome P450, and nitric oxide synthase. The section entitled Previous and Concurrent Work describes SLS research that preceded or occurred simultaneously with the research described in the following chapters.

BACKGROUND

Förster energy transfer. Förster energy transfer (FET) is one form of radiationless transfer of energy from one molecule to another.^{2,3} In order for this process to occur the donor emission and acceptor absorption spectra must overlap. FET is modeled as the interaction of the donor and acceptor dipoles, and so has an r^6 distance dependence. This process is characterized by the equations (Eqns. 1-3):

$$k_E = k_0 \left(\frac{R_0}{r} \right)^6 \quad (1)$$

$$R_0^6 = 8.8 \cdot 10^{-5} (\kappa^2 n^{-4} \phi_0 J) \quad (2)$$

$$J = \frac{\int_0^\infty F_0(\lambda)E_A(\lambda)\lambda^4 d\lambda}{\int_0^\infty F_0(\lambda)d\lambda} \quad (3)$$

Here k_E is the rate of energy transfer, k_0 is the intrinsic decay rate of the donor, r is the donor-acceptor distance, R_0 is the characteristic distance of the Förster pair, κ^2 is an orientation factor (2/3 for a freely rotating donor or acceptor), n is the index of refraction, φ_0 is the donor luminescence quantum yield, λ is wavelength (nm), $F_0(\lambda)$ is the fluorescence emission spectrum, and $E_A(\lambda)$ is the acceptor absorption spectrum ($\text{M}^{-1}\text{cm}^{-1}$).

R_0 ranges from 10 to 70 Å, a lengthscale that corresponds nicely with the dimensions of typical proteins. R_0 increases with φ_0 and the overlap integral J . J in turn increases with the overlap of the donor and acceptor emission and absorption spectra, the strength of the acceptor absorption, and λ^4 . R_0 is thus easily tailored: Blue emission, weak absorption, and a small φ_0 produce a short R_0 , while red emission, strong absorption, and a large φ_0 produce a long R_0 .

Electron Transfer. Electron transfer (ET) through a protein can occur over distances of up to 20 Å. The rate of ET can be modeled in several ways. The most general treatment is (Eqn. 4):^{4,5}

$$k_{ET} = \left(\frac{4\pi^3}{h^2 \lambda k_B T} \right)^{1/2} \mathbf{H}_{AB}^2 \exp \left[\frac{-(\Delta G^\circ + \lambda)^2}{4\lambda k_B T} \right] \quad (4)$$

The key elements influencing the ET rate are the thermodynamic driving force ΔG , the reorganization energy λ , and the electronic coupling H_{AB} . The term λ is a measure of how much the electron donor and acceptor and their surroundings must distort in order for ET to occur. Hydrophobic solvents are insensitive to changes in charge distribution, and so lead to small λ 's; polar solvents result in large λ 's. Note that the rate of ET is maximized when $\Delta G = \lambda$.

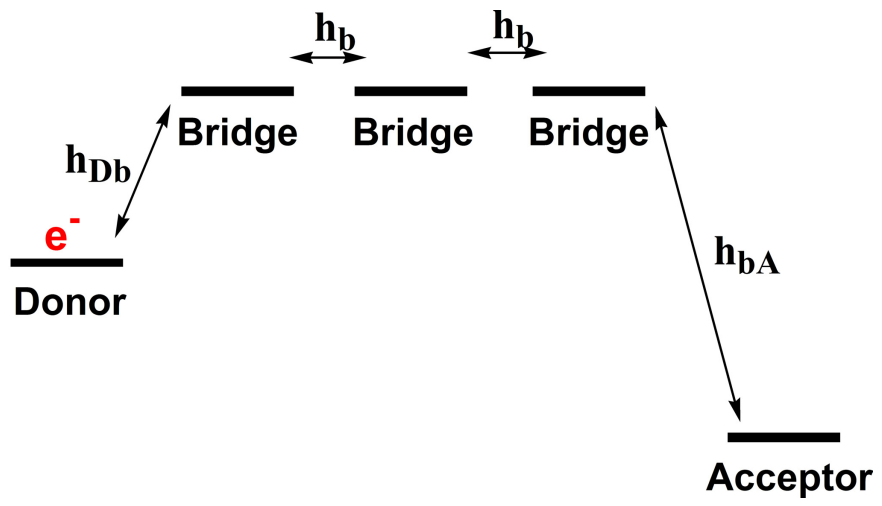
H_{AB} corresponds to the degree of electronic interaction between the donor and acceptor. In general, H_{AB} decreases exponentially with donor-acceptor spacing. Over larger distances the electronic coupling between the electron donor and acceptor is mediated by the intervening medium (Figure 1.2). It is useful to look at H_{AB} as resulting from communication across n identical bridging units (BU's), where $\Delta\varepsilon$ is the energetic gap between the donor and the unoccupied orbitals of the bridge, and h_{Db} , h_b and h_{bA} are couplings across the donor-bridge, bridge-bridge, and bridge-acceptor junctions (Eqn. 5):⁶⁻⁸

$$H_{AB} = \frac{h_{Db}}{\Delta\varepsilon} \left(\frac{h_b}{\Delta\varepsilon} \right)^{n-1} h_{bA} \quad (5)$$

Breaks in conjugation define BU boundaries. For spatially extended alkyl⁹⁻¹¹ and aromatic oligomers^{12,13} each BU decreases the ET rate by roughly a factor of 5 when $\Delta\varepsilon$ is large compared to $k_B T$. However, this simple behavior begins to break down when the

Figure 1.2. Schematic representation of superexchange-mediated electron tunneling.

The vertical dimension corresponds to the energetic potential experienced by the tunneling electron. In this simple model the bridging units are identical, and thus have identical bridge-bridge couplings and energies.

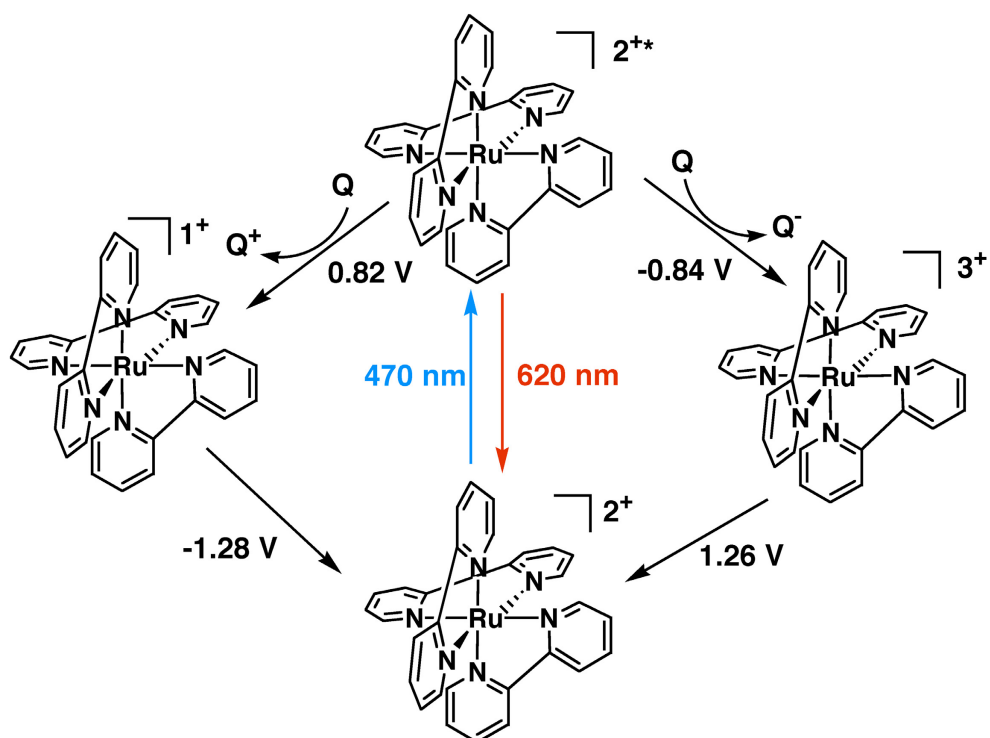


bridge is highly conjugated,^{14,15} structural dynamics control ET rates,¹⁶ or $\Delta\epsilon$ is small enough for the charge to “hop” along the bridge.¹⁷

Ruthenium tris-bipyridine. No Gray group thesis would be complete without a discussion of $[\text{Ru}(\text{bpy})_3]^{2+}$ ($\text{Ru}(\text{bpy})_3$) photophysics and chemistry (Figure 1.3). Excitation of $\text{Ru}(\text{bpy})_3$ with 470 nm light results in the promotion of an electron from the ruthenium atom to the bipyridyl ligands. This excited state has a lifetime of about a microsecond, and decays with the emission of a red photon (~620 nm) with a quantum yield of 0.042.¹⁸ The $\text{Ru}(\text{bpy})_3$ excited state is both a good oxidant (0.82 V NHE) and reductant (-0.84 V NHE). This remarkable property can be rationalized by considering the excited state to be a combination of Ru^{3+} and a bipyridine radical anion. The excited state can be intercepted with biomolecular quenchers to generate the longer-lived oxidant $[\text{Ru}(\text{bpy})_3]^{3+}$ or the reductant $[\text{Ru}(\text{bpy})_2\text{bpy}^{\cdot-}]^+$. Because of these photochemical properties, $\text{Ru}(\text{bpy})_3$ derivatives have been used extensively to study ET in proteins,⁵ and also to deliver holes and electrons to the active sites of the enzymes horseradish peroxidase¹⁹ and cytochrome *c* oxidase.^{20,21}

Ligand-protein interactions. The design of a molecule that will bind to a protein of interest may at first seem like a daunting task. However, over the past 5 years members of our research group have produced probes that bind cytochrome P450, nitric oxide synthase, amine oxidase, cytochrome *c* peroxidase, and myeloperoxidase, demonstrating

Figure 1.3. Ru(bpy)₃ photochemistry. Bimolecular reaction with a quencher (Q) can be used to generate [Ru(bpy)₃]³⁺ (1.26 V NHE) or [Ru(bpy)₂(bpy)⁻]¹⁺ (-1.28 V NHE).

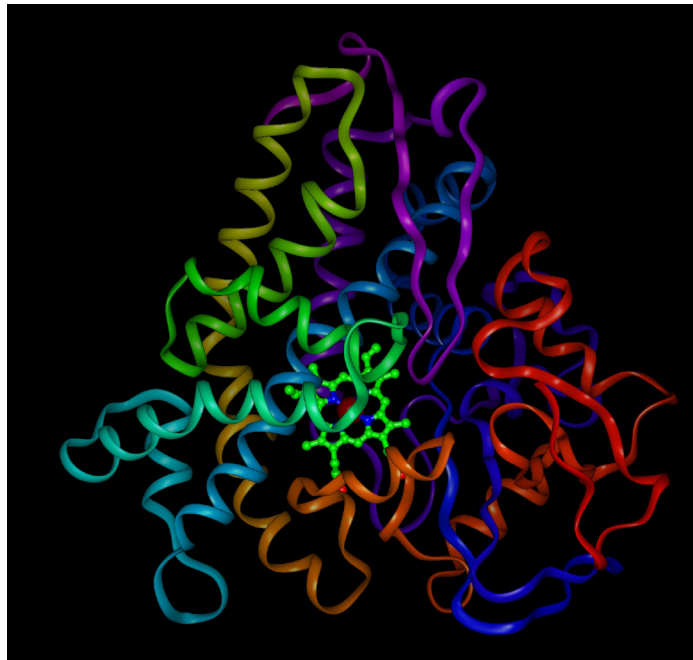


that the production of enzyme-binding photochemical probes is feasible. The simplest way to design an SLS is to elaborate upon a known substrate or inhibitor. If the crystal structure of the target enzyme is known, simple modeling greatly improves the chances of producing a probe molecule that binds to the target enzyme. While more sophisticated methods may be useful, manual docking of the proposed SLS into the active site has thus far been sufficient to uncover obvious deficiencies in probe design. Experience suggests that an iterative SLS design process is effective. It has proven far more efficient to synthesize multiple rounds of simple probe molecules than to attempt the synthesis of a more complex “optimal” SLS.

Once a functioning probe molecule exists, x-ray crystallographic determination of the structure of the probe:enzyme conjugate has proven to be very valuable. Structural characterization is helpful both in interpreting solution-phase spectroscopy and in the design of second and third generation probes. As will be discussed (Chapter 3), the structures of the probe-bound enzymes have also proven to be intrinsically interesting.

Cytochromes P450. Cytochromes P450 comprise a superfamily of heme monooxygenases characterized by a conserved fold and a cysteine-ligated heme (Figure 1.4). In particular, the ability of P450s to hydroxylate aliphatic carbon by generating a reactive heme-oxygen species has stimulated much research ($\text{R-H} + \text{O}_2 + 2\text{H}^+ + 2\text{e}^- \rightarrow \text{R-OH} + \text{H}_2\text{O}$).²² Bacteria, eukaryotes and archaeobacteria all express cytochrome P450s.²³

Figure 1.4. Ribbon diagram of cytochrome P450cam.²⁴ The fold is unique to cytochromes P450, and is highly conserved among all structurally characterized P450s despite low sequence similarities.



Cytochrome P450 genes make up a sizable fraction of expressed genes in known genomes: 0.63% in *Drosophila* (86 known genes), about 1.0% in *Arabidopsis* (270 known genes) and about 0.2% in humans (54 known genes).^{25,26}

Over 22,000 papers concerning P450 enzymes have been written in the past 10 years. This prolixity stems largely from the medical importance of these enzymes. Substrate-specific cytochromes P450 play major roles in steroid and eicosanoid biosynthesis, and thus constitute important drug design targets.²⁷⁻³¹ Inhibitors of aromatase (P450 19) have passed phase III trials in the treatment of breast cancer.²⁹ Cytochrome P450 14-sterol demethylases (CYP51) are drug targets for both antifungal agents and cholesterol lowering drugs.^{30,31}

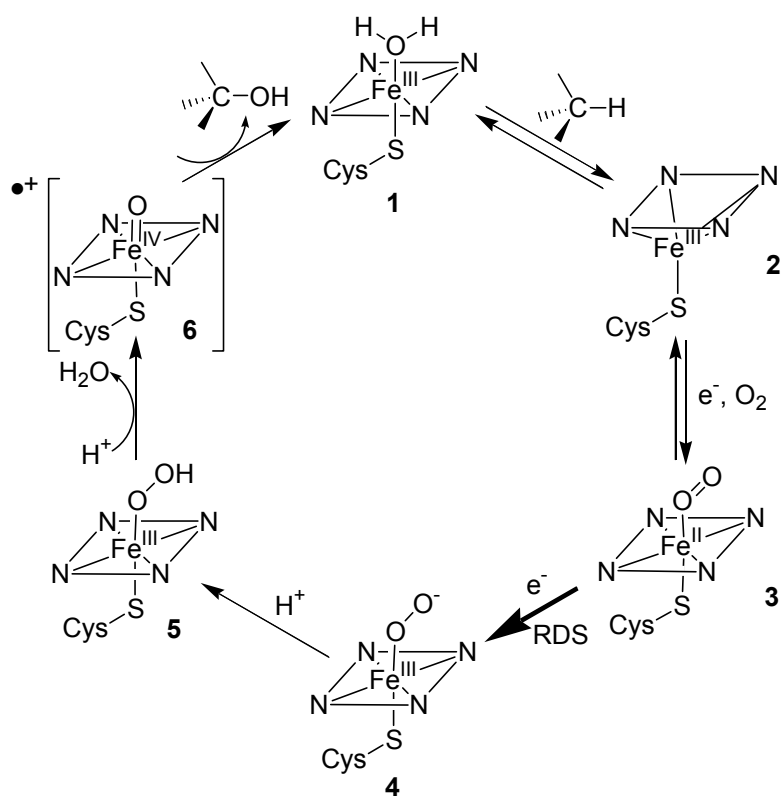
In contrast, hepatic P450s help metabolize a wide range of foreign compounds, including environmental contaminants and drugs. P450 3A4 metabolizes about half of all drugs in use.³² Although the total amount of P450's expressed varies only 3-fold in individuals, expression levels of individual P450 isozymes can vary by 1-3 orders of magnitude, leading to dramatic differences in the metabolism of xenobiotics.^{33,34} Adverse drug reactions, for instance, to Prozac,³⁵ result from individual variations in hepatic P450s.³⁶ The reactions catalyzed by cytochromes P450 are not always benign:

P450 1A2 N-hydroxylates aromatic heterocycles found in cigarette smoke and charred food, converting them into potent carcinogens.³⁷

Cytochrome P450 reaction mechanism. Both this thesis and the majority of mechanistic P450 studies employ cytochrome P450cam, a prototypical P450 from the soil bacterium *Pseudomonas putida*. The canonical P450 mechanism is shown in Figure 1.5. The steps through intermediate **3** are well established: Substrate binding displaces water from the heme iron, converting it from low-spin, six-coordinate to high-spin, five-coordinate (**2**).³⁸ The spin shift is accompanied by a change in the ferric heme reduction potential from -150 to -300 mV, which makes its reduction by putidaredoxin (Putd) thermodynamically feasible.³⁹ Dioxygen binds to the reduced heme, producing a well-characterized ferrous-dioxygen intermediate (**3**).⁴⁰

The addition of the second reducing equivalent by Putd is the last kinetically resolvable step in the catalytic cycle under biological conditions. Low-temperature ENDOR measurements indicate that reduction of **3** results in a ferric-peroxy intermediate, which rapidly protonates (**5**).⁴¹ In these experiments the next observed species is hydroxylated camphor and the resting enzyme. Based on the mechanisms of many other heme oxidases, it is assumed that the active, hydroxylating species is a ferryl cation radical (**6**) known as compound I.⁴² Recent results show that compound I can

Figure 1.5. The canonical cytochrome P450 catalytic cycle. ET constitutes the rate determining step (RDS) in catalysis under biologically relevant conditions.



indeed be generated using organic peracids.^{43,44} However, debate persists as to whether compound I, the peroxy intermediate **5**, or other species constitute the key oxidizing intermediate. Some evidence suggests that the oxidizing intermediate may be substrate and isozyme dependent.⁴⁵

Nitric oxide synthase. Nitric oxide (NO) is recognized as a ubiquitous biological second messenger, acting in a myriad of circumstances that include neuronal development, regulation of blood pressure, apoptosis, neurotransmission, and immunological response.⁴⁶⁻⁵² These diverse functions depend on the production of NO by nitric oxide synthase (NOS), an enzyme that catalyzes the transformation $L\text{-Arg} + 2\text{O}_2 + 3/2(\text{NADPH} + \text{H}^+) \rightarrow L\text{-citrulline} + \text{NO} + 2\text{H}_2\text{O} + 3/2 \text{NADP}^+$.⁵³ Like cytochrome P450, the NOS active site contains a cysteine-ligated heme. However, the active site also contains a tetrahydrobiopterin cofactor (H₄B) that is essential for catalysis.

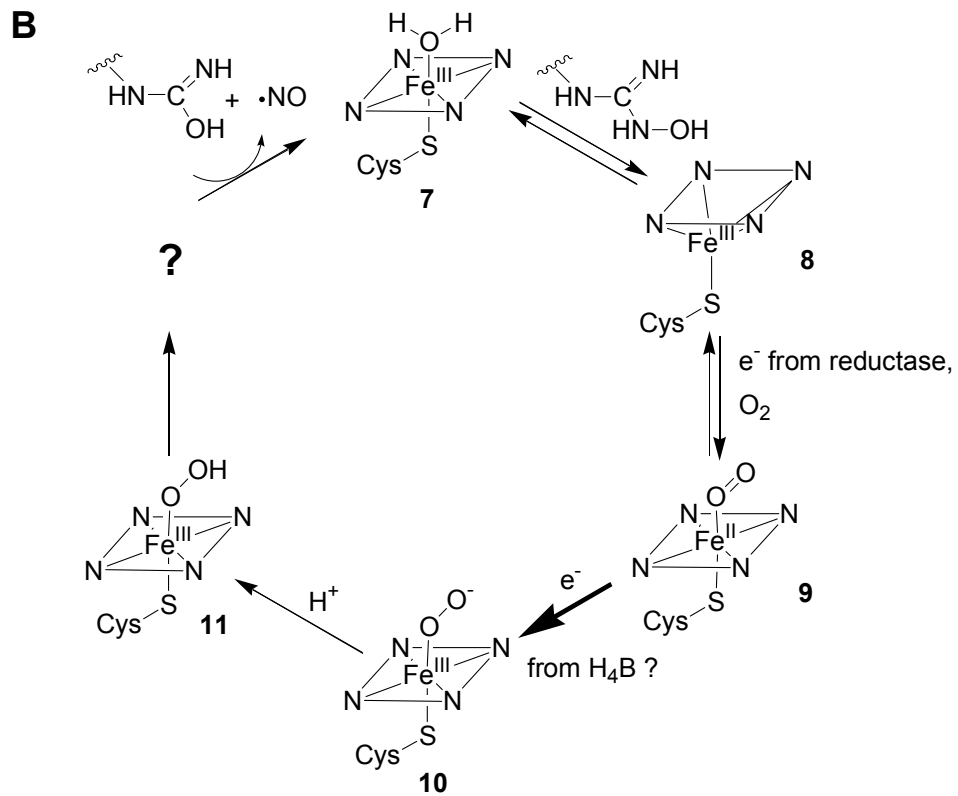
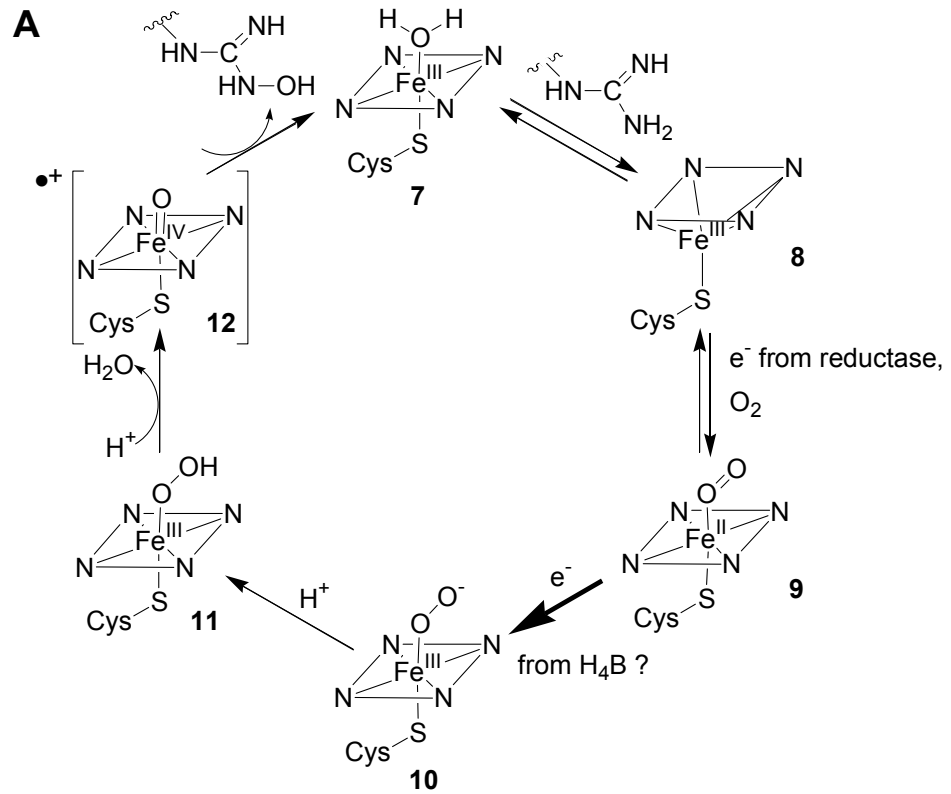
NOS was isolated independently from neuronal (nNOS), endothelial (eNOS), and immune system cells (iNOS).⁵⁴⁻⁵⁸ A more distantly related NOS has also been isolated from the bacterium *Bacillus subtilis*.⁵⁹ Subsequent research has shown that the mammalian NOS isozymes occur with a complex distribution in a wide variety of tissues. Abnormal nNOS activity has been implicated in a variety of diseases, including both Parkinson's and Alzheimer's disease.^{49,60} The isozyme eNOS is expressed in smooth muscles, including those lining blood vessels.⁴⁷ Local production of NO triggers the

relaxation of the vascular tissue, leading to a reduction in blood pressure. In addition to vasodilation, eNOS also modulates angiogenesis.⁶¹ iNOS is thought to be essential in fighting tuberculosis,⁶² but is also involved in the often destructive inflammation response to infection or injury.⁵¹

NOS reaction mechanism. The complete NOS enzyme consists of a heme-containing oxidase domain and an FMN- and FAD-containing reductase domain that are connected by a calmodulin-binding linker.^{54,63,64} The reductase domain binds NADPH and shuttles electrons into the oxidase domain. NOS functions as a dimer, with the reductase domain from one half providing electrons to the oxidase domain of the second half.^{65,66}

The catalytic mechanism of NOS is thought to be analogous to that of cytochrome P450 in many respects (Figure 1.6). Like P450, a compound I species is thought to catalyze the conversion of arginine to N-hydroxyarginine.⁶⁷ However, current evidence does not rule out other potential hydroxylating intermediates, notably ferric-peroxy species.⁶⁸ The mechanism for the oxidation of N-hydroxyarginine to citrulline and NO has been proposed to be catalyzed by ferric-peroxy or superoxy species.⁶⁸ Intriguingly, the conversion of N-hydroxyarginine to NO and citrulline formally requires oxidation by only one electron. This unusual stoichiometry has led some to suggest that the nitroxyl anion (NO^-) may be the initial product formed.⁶⁴ Current evidence suggests that H_4B

Figure 1.6. NOS catalytic mechanism. Arginine hydroxylation (A) is thought to follow a mechanism similar to that of P450. Current evidence suggests that H₄B acts as a temporary electron donor, and is presumably re-reduced by the reductase domain after catalysis is complete. The production of NO from N-hydroxyarginine (B) is poorly understood. Numerous mechanisms involving the reaction of intermediates **9**, **10**, **11** or **12** with N-hydroxyarginine have been proposed. The observation of a pterin radical during single turnover experiments suggests that a two-electron reduced oxygen intermediate such as **10**, **11** or **12** plays some part in the mechanism.



donates an electron during both catalytic cycles.⁶⁹ Despite this clear catalytic role, it is not clear why NOS requires H₄B while cytochrome P450 does not.

PREVIOUS AND CONCURRENT WORK

Ru-wires for P450cam. The original impetus for the creation of sensitizer-linked substrates was the desire to observe the fleeting intermediates in P450 catalysis (Figure 1.5). In order to observe intermediates **5** and **6**, Ivan Dmochowski *et al.* sought to use Ru(bpy)₃-functionalized P450cam substrates (Ru-wires) to rapidly reduce the ferrous dioxygen intermediate **3**, thus replacing the sluggish reduction by Putd with a rapid photochemical trigger. The initial Ru-wires investigated consist of a Ru(bpy)₃ moiety connected to adamantane, imidazole, or ethylbenzene by an alkyl linker of varying length (Figure 1.7).⁷⁰ The Ru-wires bind P450cam with micromolar K_d's, as evidenced by changes to the heme absorption spectrum and FET from the Ru-diimine excited state to the heme Q-bands (Table 1.1).⁷¹ Interestingly, neither the adamantyl nor imidazole groups are necessary for binding: Ru-wires terminating in an alkyl chain bind to the enzyme, suggesting that interactions of the enzyme with the Ru-diimine and linker moieties provide the bulk of the binding energy.

The crystal structure of Ru-C₉-Ad bound to P450cam was determined to 1.55 Å resolution by Ivan Dmochowski and Brian Crane.⁷¹ Preliminary analysis showed that a

Figure 1.7. First generation Ru-wires. The Ru(bpy)₃ photosensitizer is connected to adamantane, ethylbenzene, or the heme ligand imidazole through an alkyl chain of varying length.

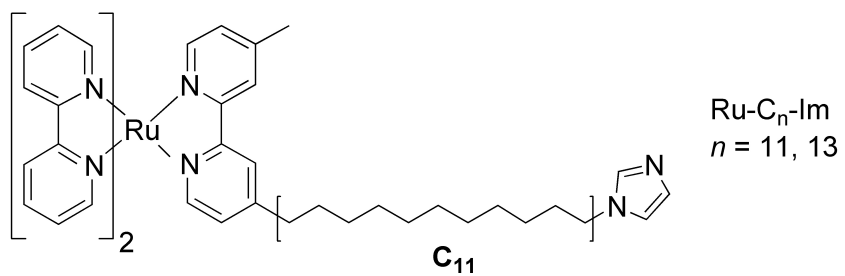
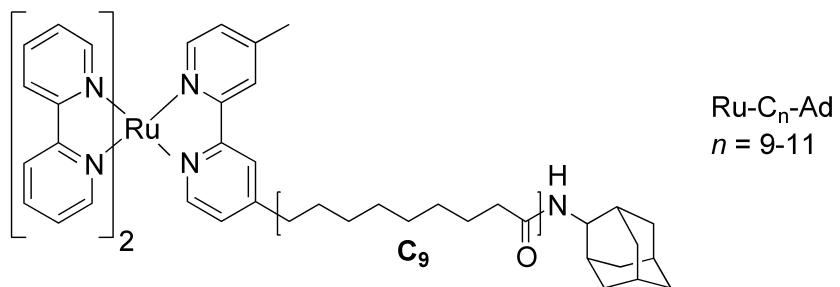
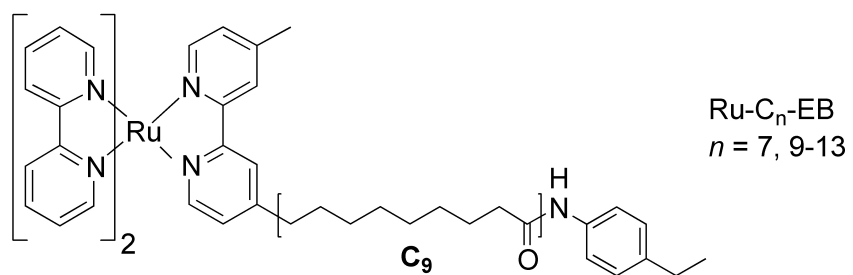


Table 1.1. Ru-wire dissociation constants and Ru-Fe distances derived from FET measurements.

Compound	K_d , μM	Ru-Fe, \AA
Ru-C ₁₃ -EB	1.7 ± 0.4	20.6 ± 0.2
Ru-C ₁₂ -EB	1.5 ± 0.3	20.5 ± 0.2
Ru-C ₁₁ -EB	0.9 ± 0.4	20.1 ± 0.3
Ru-C ₁₀ -EB	0.9 ± 0.4	19.9 ± 0.1
Ru-C ₉ -EB	0.7 ± 0.1	19.4 ± 0.1
Ru-C ₇ -EB	6.5 ± 1.3	19.5 ± 0.1
Ru-C ₉ -Ad	0.8 ± 0.3	21.0 ± 0.3
Ru-C ₁₁ -Ad	0.7 ± 0.2	21.4 ± 0.2
Ru-C ₁₃ -Im	4.1 ± 1.1	21.2 ± 0.1
Ru-C ₁₁ -Im	> 50	NA

conformational change opens a 21-Å deep channel in order to allow Ru-C₉-Ad access to the active site. The Ru-Fe distance seen in the crystal structure agrees well with that calculated from the rate of energy transfer observed in solution, demonstrating the utility of FET calculations for characterizing SLS:enzyme interactions.

The FET-derived Ru-heme distances for a series of ethylbenzene Ru-wires remains roughly constant for varying alkyl chain lengths (Table 1.1), indicating that an optimal Ru-heme distance exists in the Ru-wire:P450 conjugate.⁷¹ In contrast, Ru-C₁₃-Im binds P450cam ($K_d = 4.1 \mu\text{M}$), while Ru-C₁₁-Im does not. Evidently, the imidazole tip must ligate the heme iron in order for binding to occur, suggesting a substantial energetic penalty for its sequestration in the hydrophobic P450 active site. This result demonstrates that sensitive binding discrimination is possible with properly designed probe molecules.

As synthesized, the Ru-wires consist of a racemic mixture of Δ and Λ stereoisomers. However, the Δ and Λ forms of Ru-C₉-Ad were successfully separated using chiral chromatography. The isomers bind P450cam with similar dissociation constants ($K_d(\Delta) = 190 \text{ nM}$; $K_d(\Lambda) = 90 \text{ nM}$), corresponding to a difference in binding energies of $0.46 \text{ kcal mol}^{-1}$.⁷² Detailed analysis shows that the apparent K_d for the racemate is not the average of the stereoisomer K_d 's.⁷³

P450cam hydroxylates Ru-C₉-Ad when supplied with electrons via the natural NADH/putidaredoxin reductase/Putd reduction relay.⁷⁴ Ru-C₉-Ad hydroxylation occurs

at only 1.6% the rate of camphor hydroxylation, and only 10% of the electrons supplied by NADH go to product formation. Presumably the rest are diverted to the formation of reduced oxygen species such as superoxide or hydrogen peroxide.⁷⁵ The ability of P450cam to hydroxylate a molecule so structurally different from camphor is remarkable. As discussed in Chapter 3, Ru-wire turnover supports the hypothesis that the structural flexibility inherent in the P450 fold allows cytochromes P450 to hydroxylate structurally diverse substrates.

Photochemically reduced or oxidized Ru-wires transfer electrons or holes to the P450cam ferric heme with time constants of around 50 μ s (Figures 1.8, 1.9),⁷⁰ rates that are typical for ET through saturated bonds over comparable distances. These results demonstrate that it is in principle possible to trigger reactions in the buried active sites of proteins on the sub-millisecond timescale.

Dual SLS and enzyme engineering: cytochrome *c* peroxidase. The removal of the residues thought to mediate ET to the heme of cytochrome *c* peroxidase (CCP) results in a ligand-binding channel (Figure 1.10).⁷⁶ Hays *et al.* describe a dansyl-functionalized peptide that binds within this channel (Figure 1.11).⁷⁷ Partial unfolding and renaturation of the CCP mutant in the presence of **13** or **14** results in the kinetic trapping of the peptide within the channel. In contrast to cytochrome P450, peptide binding depends crucially on the replication of hydrogen bonding and salt bridging interactions present in

Figure 1.8. The flash-quench sequence for delivering electrons or holes into the active site of P450cam. The Ru-wire is excited with 470 nm light (Ru^*), and intercepted with either $\text{Co}(\text{NH}_3)_6^{3+}$ or *para*-methoxy-N,N-dimethylaniline (PMDA) to generate the oxidized (Ru^{3+}) or reduced (Ru^{1+}) Ru-wire. The photochemically generated hole or electron tunnels to the heme on the millisecond timescale, forming a heme cation radical or ferrous heme.

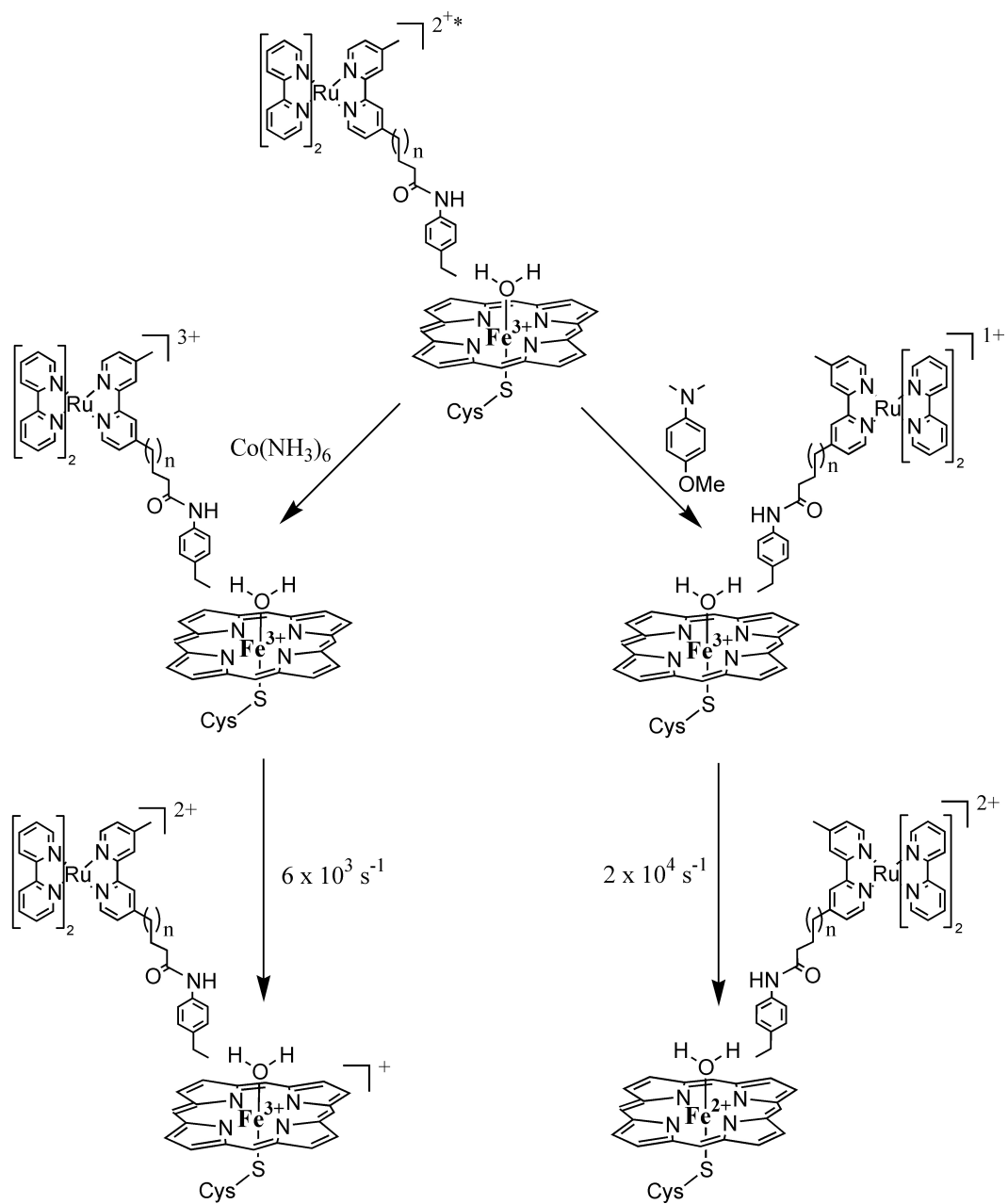


Figure 1.9. Transient absorption difference kinetics showing the reduction of P450cam by photochemically generated $[\text{Ru}^{\text{I}}\text{-C}_{13}\text{-Im}]^+$ (10 μM Ru-C₁₃-Im, 20 μM P450cam, 20 mM PMDA). Figure from ref. 73 (used with permission).

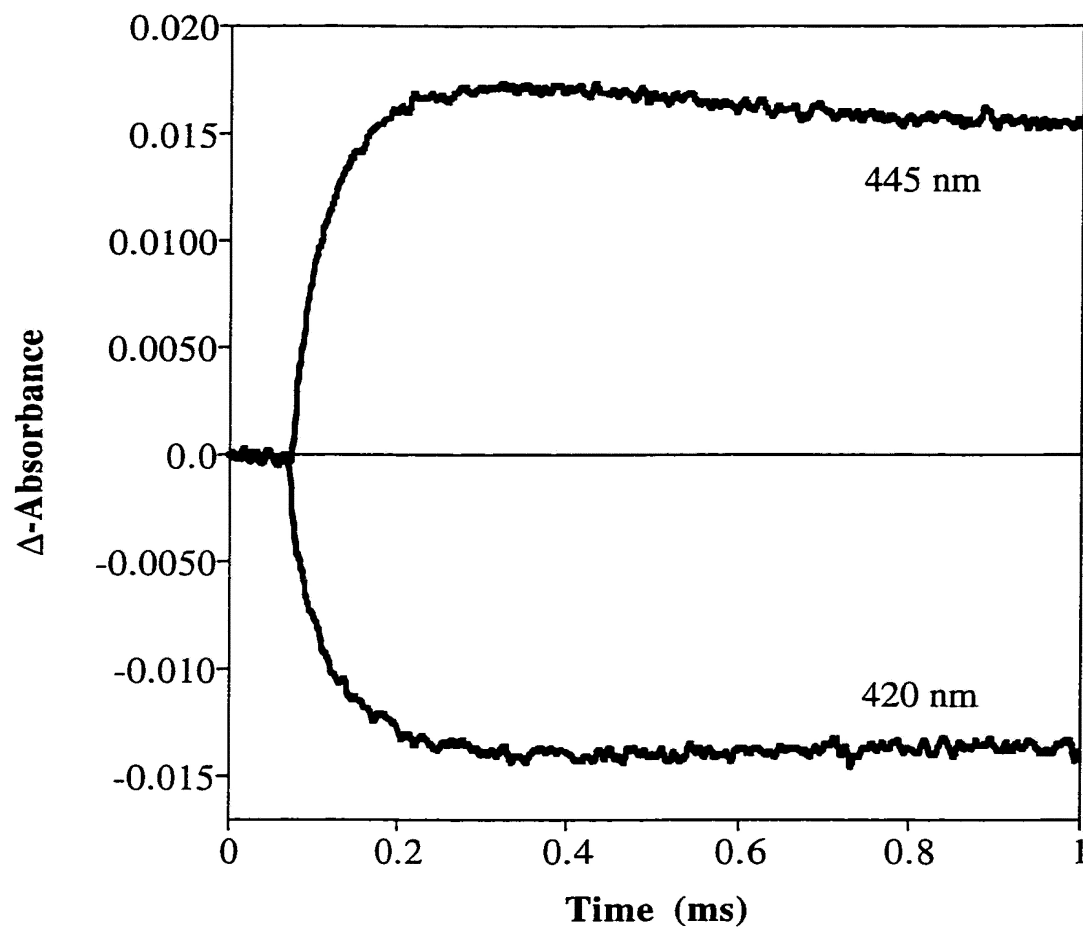


Figure 1.10. Crystal structure of the channel-containing CCP mutant (blue) overlaid with wild-type CCP (white). The mesh shows the surface of the protein, including the channel that reaches deep into the enzyme. The deleted residues are shown in cyan.

Figure provided by Anna-Maria A. Hays.

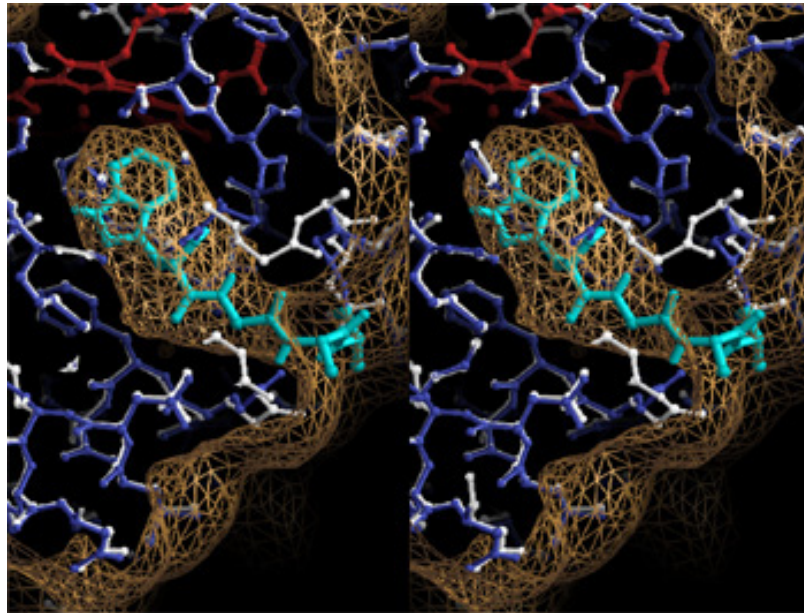
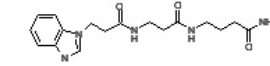
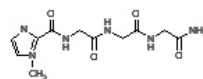
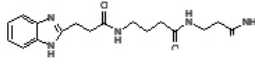
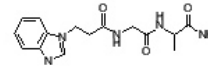
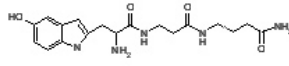
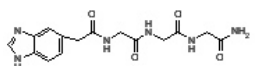
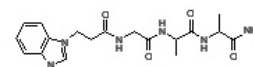
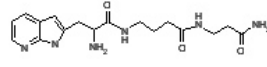
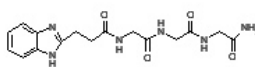
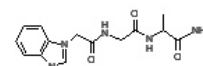
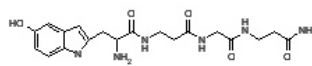
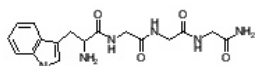
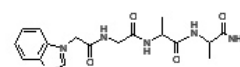
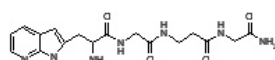
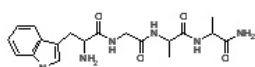
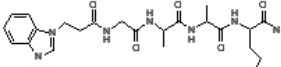
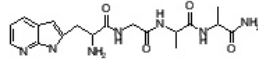
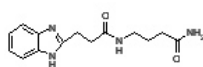


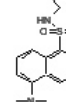
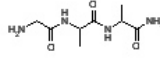
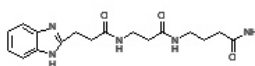
Figure 1.11. Amide oligomers designed to bind in the artificial CCP channel. Only **13** and **14**, which mimic the hydrogen-bonding pattern of the native peptide, bind to the enzyme. Figure provided by Anna-Maria A. Hays.



13



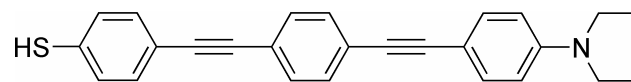
14



the native enzyme. These observations demonstrate that not all enzymes possess the structural flexibility of cytochrome P450 (Chapter 3).

Electrochemistry at a deeply buried active site: amine oxidase. The enzyme amine oxidase (AO) catalyzes the conversion of amines to aldehydes and ammonia using an active site that contains both copper and a topoquinone cofactor. The catalytic role of copper (if any) in catalysis remains a matter of persistent debate. The potentials of the deeply buried topoquinone and copper cannot be accurately measured using conventional electrochemical techniques. Instead, Hess *et al.* measured the topoquinone potential using gold electrodes functionalized with a phenyl-alkynyl bridge designed to bind in the AO active site, thus providing an ET conduit from the electrode to the topoquinone (Figure 1.12).⁷⁸ The topoquinone potential was found to be -360 mV, and no copper electrochemistry was observed. However, it is not clear whether the copper potential is anomalously low or if it could not be measured due to weak electronic coupling with the phenyl-alkynyl bridge.

Figure 1.12. The highly conjugated molecular “wire” used to electronically couple the active site of amine oxidase to a gold electrode. N,N-diethylaniline is a known inhibitor of amine oxidase.



REFERENCES

- (1) Moerner, W. E.; Orrit, M. *Science* **1999**, *283*, 1670-1676.
- (2) Wu, P. G.; Brand, L. *Anal. Biochem.* **1994**, *218*, 1-13.
- (3) Foerster, T. *Ann. Phys.-Berlin* **1948**, *2*, 55-75.
- (4) Marcus, R. A. *J. Chem. Phys.* **1956**, *24*, 966-978.
- (5) Gray, H. B.; Winkler, J. R. *Annu. Rev. Biochem.* **1996**, *65*, 537-561.
- (6) McConnell, H. *J. Chem. Phys.* **1961**, *35*, 508-515.
- (7) Davis, W. B.; Wasielewski, M. R.; Ratner, M. A.; Mujica, V.; Nitzan, A. *J. Phys. Chem. A* **1997**, *101*, 6158-6164.
- (8) Davis, W. B.; Ratner, M. A.; Wasielewski, M. R. *Chem. Phys.* **2002**, *281*, 333-346.
- (9) Yonemoto, E. H.; Saupe, G. B.; Schmehl, R. H.; Hubig, S. M.; Riley, R. L.; Iverson, B. L.; Mallouk, T. E. *J. Am. Chem. Soc.* **1994**, *116*, 4786-4795.
- (10) Smalley, J. F.; Feldberg, S. W.; Chidsey, C. E. D.; Linford, M. R.; Newton, M. D.; Liu, Y. P. *J. Phys. Chem.* **1995**, *99*, 13141-13149.
- (11) Paddon-Row, M. N.; Oliver, A. M.; Warman, J. M.; Smit, K. J.; De Haas, M. P.; Oevering, H.; Verhoeven, J. W. *J. Phys. Chem.* **1988**, *92*, 6958-6962.
- (12) Helms, A.; Heiler, D.; McLendon, G. *J. Am. Chem. Soc.* **1992**, *114*, 6227-6238.

- (13) Creager, S.; Yu, C. J.; Bamdad, C.; O'Connor, S.; MacLean, T.; Lam, E.; Chong, Y.; Olsen, G. T.; Luo, J. Y.; Gozin, M.; Kayyem, J. F. *J. Am. Chem. Soc.* **1999**, *121*, 1059-1064.
- (14) Sikes, H. D.; Smalley, J. F.; Dudek, S. P.; Cook, A. R.; Newton, M. D.; Chidsey, C. E. D.; Feldberg, S. W. *Science* **2001**, *291*, 1519-1523.
- (15) Davis, W. B.; Svec, W. A.; Ratner, M. A.; Wasielewski, M. R. *Nature* **1998**, *396*, 60-63.
- (16) Davis, W. B.; Ratner, M. A.; Wasielewski, M. R. *J. Am. Chem. Soc.* **2001**, *123*, 7877-7886.
- (17) Kilsa, K.; Kajanus, J.; Macpherson, A. N.; Martensson, J.; Albinsson, B. *J. Am. Chem. Soc.* **2001**, *123*, 3069-3080.
- (18) Roundhill, D. M. *Photochemistry and Photophysics of Metal Complexes*; Plenum Press: New York, 1994.
- (19) Berglund, J.; Pascher, T.; Winkler, J. R.; Gray, H. B. *J. Am. Chem. Soc.* **1997**, *119*, 2464-2469.
- (20) Zaslavsky, D.; Kaulen, A. D.; Smirnova, I. A.; Vygodina, T.; Konstantinov, A. A. *FEBS Lett.* **1993**, *336*, 389-393.
- (21) Zaslavsky, D.; Sadoski, R. C.; Wang, K. F.; Durham, B.; Gennis, R. B.; Millett, F. *Biochemistry* **1998**, *37*, 14910-14916.

- (22) Ortiz de Montellano, P. R., Ed. *Cytochrome P450: Structure, Mechanism, and Biochemistry*; Plenum Press: New York, 1995.
- (23) McLean, M.; Maves, S.; Weiss, K. E.; Krepich, S.; Sligar, S. G. *Biochem. Biophys. Res. Commun.* **1998**, *252*, 166-172.
- (24) Poulos, T. L.; Finzel, B. C.; Howard, A. J. *J. Mol. Biol.* **1987**, *195*, 867-700.
- (25) Nelson, D. R. *Arch. Biochem. Biophys.* **1999**, *369*, 1-10.
- (26) Nelson, D. R. (2002) Cytochrome P450 homepage:
<http://drnelson.utmem.edu/CytochromeP450.html>
- (27) Kagawa, N.; Waterman, M. R. In *Cytochrome P450: Structure, Mechanism, and Biochemistry*; Ortiz de Montellano, P. R., Ed.; Plenum Press: New York, 1995, pp 419-442.
- (28) Capdevila, J. H.; Zeldin, D.; Makita, K.; Karara, A.; Falck, J. R. In *Cytochrome P450: Structure, Mechanism and Biochemistry*; Ortiz de Montellano, P. R., Ed.; Plenum Press: New York, 1995, pp 443-472.
- (29) Goss, P. E.; Strasser, K. *J. Clin. Oncol.* **2001**, *19*, 881-894.
- (30) Frye, L. L.; Leonard, D. A. *Crit. Rev. Biochem. Mol. Biol.* **1999**, *34*, 123-140.
- (31) Sheehan, D. J.; Hitchcock, C. A.; Sibley, C. M. *Clin. Microbiol. Rev.* **1999**, *12*, 40-79.
- (32) Guengerich, F. P. *Annu. Rev. Pharmacol. Toxicol.* **1999**, *39*, 1-17.

- (33) Disterath, L. M.; Guengerich, F. P., Eds. *Enzymology of Human Liver Cytochromes P-450*; CRC Press: Boca Raton, FL, 1987; Vol. 1.
- (34) Guengerich, F. P. In *Cytochrome P450: Structure, Mechanism and Biochemistry*; Ortiz de Montellano, P. R., Ed.; Plenum Press: New York, NY, 1995, pp 473-536.
- (35) Otton, S. V.; Wu, D. F.; Joffe, R. T.; Cheung, S. W.; Sellers, E. M. *Clin. Pharm. Ther.* **1993**, *53*, 401-409.
- (36) Li, A. P., Ed. *Drug-drug interactions: scientific and regulatory perspectives*; Academic Press: New York, 1997.
- (37) Lang, N. P.; Butler, M. A.; Massengill, J.; Lawson, M.; Stotts, R. C.; Hauerjensen, M.; Kadlubar, F. F. *Cancer Epidemiol. Biomarkers Prev.* **1994**, *3*, 675-682.
- (38) Sligar, S. G. *Biochemistry* **1976**, *15*, 5399-5406.
- (39) Sligar, S. G.; Gunsalus, I. C. *Proc. Natl. Acad. Sci. U.S.A.* **1976**, *73*, 1078-1082.
- (40) Schlichting, I.; Berendzen, J.; Chu, K.; Stock, A. M.; Maves, S. A.; Benson, D. E.; Sweet, R. M.; Ringe, D.; Petsko, G. A.; Sligar, S. G. *Science* **2000**, *287*, 1615-1622.
- (41) Davydov, R.; Makris, T. M.; Kofman, V.; Werst, D. E.; Sligar, S. G.; Hoffman, B. M. *J. Am. Chem. Soc.* **2001**, *123*, 1403-1415.
- (42) Groves, J. T.; McClusky, G. A.; White, R. E.; Coon, M. J. **1978**, *81*, 154-160.
- (43) Kellner, D. G.; Hung, S. C.; Weiss, K. E.; Sligar, S. G. *J. Biol. Chem.* **2002**, *277*, 9641-9644.

- (44) Egawa, T.; Shimada, H.; Ishimura, Y. *Biochem. Biophys. Res. Commun.* **1994**, *201*, 1464-1469.
- (45) Ortiz de Montellano, P. R.; De Voss, J. J. *Nat. Prod. Rep.* **2002**, *19*, 477-493.
- (46) Kendrick, K. M.; Guzman, R. G.; Zorrilla, J.; Hinton, M. R.; Broad, K. D.; Mimmack, M.; Okura, S. *Nature* **1997**, *388*, 670-674.
- (47) Huang, P. L.; Huang, H. H.; Mashimo, H.; Bloch, K. D.; Moskowitz, M. A.; Bevan, J. A.; Fishman, M. C. *Nature* **1995**, *377*, 239-242.
- (48) Ko, G. Y.; Kelly, P. T. *J. Neurosci.* **1999**, *19*, 6784-6794.
- (49) Luth, H. J.; Holzer, M.; Gertz, H. J.; Arendt, T. *Brain Res.* **2000**, *852*, 45-55.
- (50) Mize, R. R.; Dawson, T. M.; Dawson, V. L.; Friedlander, M. J. *Nitric Oxide in Brain Development, Plasticity and Disease*; Elsevier, 1998.
- (51) Nathan, D. *J. Clin. Invest.* **1997**, *100*, 2417-2423.
- (52) Lancaster, J. *Nitric Oxide: Principles and Actions*; Academic Press: San Diego, CA, 1996.
- (53) Stuehr, D. J. *Biochim. Biophys. Acta* **1999**, *1411*, 217-230.
- (54) Bredt, D. S.; Hwang, P. M.; Glatt, C. E.; Lowenstein, C.; Reed, R. R.; Snyder, S. H. *Nature* **1991**, *351*, 714-718.
- (55) Janssens, S. P.; Simouchi, A.; Quertermous, T.; Bloch, D. B.; Bloch, K. D. *J. Biol. Chem.* **1992**, *267*, 22694.

- (56) Lamas, S.; Marsden, P. A.; Li, G. K.; Tempst, P.; Mickel, T. *Proc. Natl. Acad. Sci. U.S.A.* **1992**, *89*, 6348-6352.
- (57) Lowenstein, C. J.; Glatt, C. S.; Brecht, D. S.; Snyder, S. H. *Proc. Natl. Acad. Sci. U.S.A.* **1992**, *89*, 6711-6715.
- (58) Xie, Q. W.; Cho, H. J.; Calaycay, J.; Mumford, R. A.; Swiderek, K. M.; Lee, T. D.; Ding, A.; Troso, T.; Nathan, C. *Science* **1992**, *256*, 225-228.
- (59) Pant, K.; Bilwes, A. M.; Adak, S.; Stuehr, D. J.; Crane, B. R. *Biochemistry* **2002**, *41*, 11071-11079.
- (60) Dawson, V. L.; Dawson, T. M. *Prog. Brain Res.* **1998**, *118*, 215-229.
- (61) Dimmeler, S.; Zeiher, A. M. *Cell Death Differ.* **1999**, *6*, 964-968.
- (62) MacMicking, J. D.; North, R. J.; LaCourse, R.; Mudgett, J. S.; Shah, S. K.; Nathan, C. F. *Proc. Natl. Acad. Sci. U.S.A.* **1997**, *94*, 5243-5248.
- (63) Cho, H. J.; Xie, Q. W.; Calaycay, J.; Mumford, R. A.; Swiderek, K. M.; Lee, T. D.; Nathan, C. *J. Exp. Med.* **1992**, *176*, 599-604.
- (64) Alderton, W. K.; Cooper, C. E.; Knowles, R. G. *Biochem. J.* **2001**, *357*, 593-615.
- (65) Siddhanta, U.; Wu, C. Q.; Abu-Soud, H. M.; Zhang, J. L.; Ghosh, D. K.; Stuehr, D. J. *J. Biol. Chem.* **1996**, *271*, 7309-7312.
- (66) Crane, B. R.; Rosenfeld, R. J.; Arvai, A. S.; Ghosh, D. K.; Ghosh, S.; Tainer, J. A.; Stuehr, D. J.; Getzoff, E. D. *EMBO J.* **1999**, *18*, 6271-6281.

- (67) Rosen, G. M.; Tsai, P.; Pou, S. *Chem. Rev.* **2002**, *102*, 1191-1199.
- (68) Davydov, R.; Ledbetter-Rogers, A.; Martasek, P.; Larukhin, M.; Sono, M.; Dawson, J. H.; Masters, B. S. S.; Hoffman, B. M. *Biochemistry* **2002**, *41*, 10375-10381.
- (69) Wei, C. C.; Wang, Z. Q.; Wang, Q.; Meade, A. L.; Hemann, C.; Hille, R.; Stuehr, D. J. *J. Biol. Chem.* **2001**, *276*, 315-319.
- (70) Wilker, J. J.; Dmochowski, I. J.; Dawson, J. H.; Winkler, J. R.; Gray, H. B. *Angew. Chem. Int. Ed. Eng.* **1999**, *38*, 90-92.
- (71) Dmochowski, I. J.; Crane, B. R.; Wilker, J. J.; Winkler, J. R.; Gray, H. B. *Proc. Natl. Acad. Sci. USA* **1999**, *96*, 12987-12990.
- (72) Dmochowski, I. J.; Winkler, J. R.; Gray, H. B. *J. Inorg. Biochem.* **2000**, *81*, 221-228.
- (73) Dmochowski, I. J. In *Chemistry and Chemical Engineering*; California Institute of Technology: Pasadena, CA, 2000.
- (74) Dmochowski, I. J.; Dunn, A. R.; Wilker, J. J.; Crane, B. R.; Green, M. T.; Dawson, J. H.; Sligar, S. G.; Winkler, J. R.; Gray, H. B. *Methods Enzymol.* **2002**, *357*, 120-133.
- (75) Sligar, S. G.; Lipscomb, J. D.; Debrunner, P. G.; Gunsalus, I. C. *Biochem. Biophys. Res. Commun.* **1974**, *61*, 290-296.

- (76) Rosenfeld, R. J.; Hays, A.-M. A.; Musah, R. A.; Goodin, D. B. *Protein Sci.* **2002**, *11*, 1251-1259.
- (77) Hays, A.-M. A.; Gray, H. B.; Goodin, D. B. *Protein Sci.* **2003**, *12*, 278-287.
- (78) Hess, C. R. In *Chemistry and Chemical Engineering*; California Institute of Technology: Pasadena, 2002.